[Original Paper]

Simulation Analysis of Multislice Profiles in MRI Based on Bloch Equation

Takashi SAKAI, Kojiro YAMAGUCHI[†], Eizo UMEZAWA[†], Koichi MUTO[†], Yuya MURAMATSU,
Yoshiyuki TAKAHASHI[††], Sachiko UEOKU[†††], Shouichi SUZUKI[††], and Kazuhiro KATADA[††††]

Fujita Health University Graduate School of Health Science
1-98, Dengakugakubo, Kutsukake, Toyoake, Aichi 470-1192, Japan
[†]Fujita Health University School of Health Science
1-98, Dengakugakubo, Kutsukake, Toyoake, Aichi 470-1192, Japan
[††]Ibaragi Prefectural University Graduate School of Health Science
2−4669, Ami, Inashiki, Ibaraki 300-0394, Japan
[†††]Toshiba Medical Systems Corporation
1-4-12, Naekiminai, Nakamuraku, Nagoya, Aichi 450-0003, Japan
[††††]Department of Radiology, Fujita Health University School of Medicine
1-98, Dengakugakubo, Kutsukake, Toyoake, Aichi 470-1192, Japan
(Received on March 22, 2006, in final form April 28, 2006)

Abstract : Interslice sensitivity variation in magnetic resonance imaging (MRI) is said to be attributable to crosstalk. Crosstalk is a phenomenon in which deterioration of the rectangular profile of the RF pulse frequency characteristics leads to poor slice profiles, resulting in interference between slices. In the present study, the ideal characteristics of multislice profiles were analyzed through numerical simulation with the Bloch equation using sinc symmetrical RF pulses. The effects of the slice excitation order on the slice profile were also examined, comparing interleaved acquisition and sequential acquisition. The results of the simulation showed that the order of image acquisition affects the slice profile.
Key words : MRI, RF pulse, crosstalk, slice profile, Bloch equation

1. Introduction

Interslice sensitivity variation in multislice magnetic resonance imaging (MRI) is said to be attributable to crosstalk. The main cause of such crosstalk is deterioration of the RF pulse adversely affecting the slice profiles [1-3]. Crosstalk effects are usually reduced by performing interleaved acquisition in which only the odd-numbered slices (1st, 3rd, 5th, 7th, 9th, 11th, 13th,...) are excited first, followed by the even-numbered slices (2nd, 4th, 6th, 8th, 10th, 12th,...) [4].

When it is preferable to employ sequential acquisition rather than interleaved acquisition due to the objectives of a particular study, it is necessary to address the issue of image deterioration due to crosstalk in sequential acquisition. Nevertheless, there have been only a few studies that have investigated the deterioration of the slice profile in multislice acquisition, comparing interleaved acquisition and sequential acquisition. In addition, there has recently been increasing clinical demand for wide-area, thin-slice image acquisition with a shorter TE.

In the present study, the effects of the π value of the RF pulse along with a shorter TE on the slice profiles were investigated in interleaved acquisition and sequential acquisition. Numerical simulation was performed under ideal conditions using the Bloch equation [5-7] to evaluate the differences between these acquisition methods.

2. Methods

2.1 Evaluation methods and evaluation position

The pulse sequence diagram used in the simulation analysis is shown in Fig. 1. The RF pulses evaluated were symmetrical
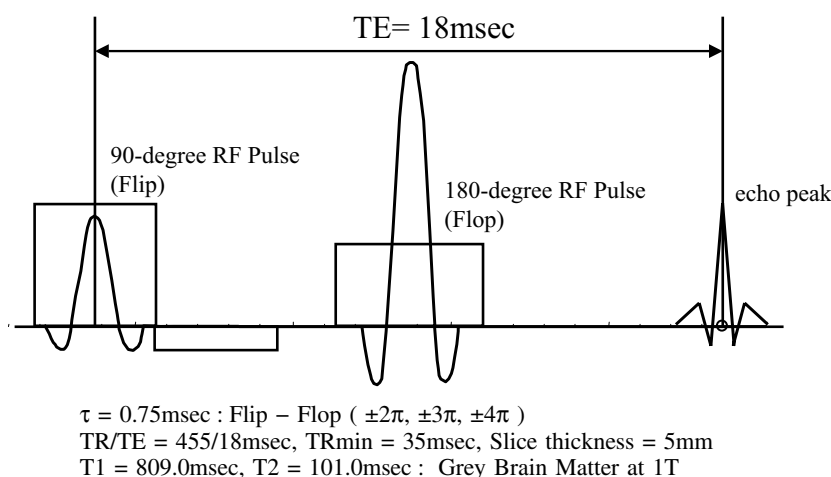

$\tau = 0.75$msec : Flip − Flop ($\pm 2\pi$, $\pm 3\pi$, $\pm 4\pi$)
TR/TE = 455/18msec, TRmin = 35msec, Slice thickness = 5mm
T1 = 809.0msec, T2 = 101.0msec : Grey Brain Matter at 1T

Fig.1 Pulse sequence diagram and analytical conditions in simulation analysis.

医用画像情報学会雑誌

sinc RF pulses [8-10]. The π values of the RF pulses were ±2π, ±3π, and ±4π for both 90° and 180°. The TE was held constant at 18 msec regardless of the π value.

The results were evaluated based on the in-plane signal values and phase angle dispersions defined as follows.

$$\text{in-plane signal value} = \sqrt{(\sum_{i=1}^{N} Mxi)^2 + (\sum_{i=1}^{N} Myi)^2} \ , \quad (1)$$

$$\text{phase angle dispersion} = \sqrt{\frac{1}{N} \sum_{i=1}^{N} (\bar{\phi} - \phi_i)^2} \ , \quad (2)$$

where $\sum_{i=1}^{N}$ denotes the summation with respect to all magnetization vectors in each slice, Mxi's and Myi's denote x and y components (transverse components) of the i-th magnetization vectors, respectively, and

$$\phi_i = \tan^{-1} \frac{Myi}{|Mxi|} \ , \quad (3)$$

$$\bar{\phi} = \frac{\sum_{i=1}^{N} \phi_i}{N} \ . \quad (4)$$

The phase angle dispersion defined by Eq. (2) represents the degree of variation in each slice. In addition, slice profiles were evaluated based on $Mxyi = \sqrt{Mxi^2 + Myi^2}$ in the echo time.

The results obtained were evaluated in reference to various baseline values in single-slice acquisition.

2.2 Simulation conditions

Two sets of simulation parameters were employed. In the first set, the interslice gap (gap) was held constant at 20% and the number of slices (NS) was varied, with values of 1, 3, 5, 7, and 13. In the second set, the NS was held constant at 13 and the gap was changed, with values of 20% and 100%. In either case, excitation was applied for both interleaved acquisition and sequential acquisition. In addition, the effect of the slice excitation order was evaluated on the Mxy slice profile in the echo time when the NS was 13.

Other simulation parameters were held constant: τ = 0.75 msec, TR/TE = 455/18 msec, TRmin = 35msec, and slice thickness = 5mm. Here, TRmin means the time required to excite one slice. T1 and T2 values were obtained from gray matter at 1 T (T1 = 809.0 msec, T2 = 101.0 msec) [11]. In addition, the 180° gradient field strength at each π was optimized in advance.

3. Results

3.1 Results for the effects of NS

The in-plane signal values for various NS values are shown in Table 1. When the NS was increased, the in-plane signal value decreased than single-slice. For all NS values, the effect of the slice excitation order was almost the same in interleaved acquisition and sequential acquisition, but interleaved acquisition showed slightly higher in-plane signal values. However, the standard deviation (SD) was higher in interleaved acquisition than in sequential acquisition. In addition, for all NS values, a high in-plane signal value was observed at ±3π, approaching the single-slice in-plane signal value.

The phase angle dispersions for various NS values are shown in Table 2. When the NS was increased, the phase angle dispersion tended to increase. As was the case for the in-plane signal value, for all NS values, when interleaved acquisition and sequential acquisition were compared, the former showed slightly greater phase angle dispersion. Furthermore, as was found for the in-plane signal value, for all NS values, the phase angle dispersion at ±3π approached the single-slice phase angle dispersion.

3.2 Results for the effects of gap

The in-plane signal values for different gaps are shown in Table 3. When the gap was set to 100%, the in-plane signal value approached the single-slice in-plane signal value. On the other hand, when the gap was set to 20%, the in-plane signal value was lower than that for a gap of 100%. In addition, for either gap, the in-plane signal value was higher at ±3π than at

Table 1 In-plane signal values for various numbers of slices (gap = 20%)

| SEP | slice | in-plane signal | | | |
| | | interleaved | | sequential | |
		mean	SD	mean	SD
±2π	single slice	771.08	—	771.08	—
	3 slice	723.17	81.31	717.97	46.37
	5 slice	714.41	75.61	706.73	35.27
	7 slice	712.90	70.31	701.90	30.87
	13 slice	715.05	60.07	696.00	21.53
±3π	single slice	779.92	—	779.92	—
	3 slice	758.42	37.28	758.33	19.15
	5 slice	754.47	34.76	753.96	14.65
	7 slice	754.72	31.08	751.86	12.47
	13 slice	755.81	26.70	749.48	9.30
±4π	single slice	747.85	—	747.85	—
	3 slice	725.40	36.52	721.04	21.50
	5 slice	722.48	32.06	722.48	32.06
	7 slice	715.33	38.26	712.76	14.27
	13 slice	717.44	32.04	710.02	10.41

Table 2 Phase angle dispersion for variues numbers of slices (gap = 20%)

| SEP | slice | Phase angle dispersion | | | |
| | | interleaved | | sequential | |
		mean	SD	mean	SD
±2π	single slice	2.54	—	2.54	—
	3 slice	4.80	0.40	4.43	1.22
	5 slice	5.34	1.94	4.80	1.04
	7 slice	5.15	0.54	4.90	0.84
	13 slice	4.93	0.80	4.93	0.62
±3π	single slice	1.76	—	1.76	—
	3 slice	2.90	0.26	2.65	0.72
	5 slice	3.18	0.97	2.85	0.59
	7 slice	3.12	0.40	2.93	0.49
	13 slice	3.10	0.55	3.02	0.37
±4π	single slice	2.20	—	2.20	—
	3 slice	4.42	1.58	3.96	0.55
	5 slice	5.58	3.70	5.58	3.70
	7 slice	4.12	1.26	4.11	1.10
	13 slice	3.76	0.72	4.20	0.88

Table 3 In-plane signal values for different interslice gaps (NS = 13)

SEP	Gap	in-plane signal			
		interleaved		sequential	
		mean	SD	mean	SD
±2π	single slice	771.08	—	771.08	—
	20%	715.05	60.07	696.00	21.53
	100%	767.30	3.30	766.71	1.87
±3π	single slice	779.92	—	779.92	—
	20%	755.81	26.70	749.48	9.30
	100%	779.24	0.84	779.09	0.35
±4π	single slice	747.85	—	747.85	—
	20%	717.44	32.04	710.02	10.41
	100%	745.63	1.60	745.44	1.49

Table 4 Phase angle dispersion for different interslice gaps (NS = 13)

SEP	Gap	Phase angle dispersion			
		interleaved		sequential	
		mean	SD	mean	SD
±2π	single slice	2.54	—	2.54	—
	20%	4.93	0.80	4.93	0.62
	100%	4.63	0.63	4.65	0.65
±3π	single slice	1.76	—	1.76	—
	20%	3.10	0.55	3.02	0.37
	100%	2.90	0.38	2.91	0.38
±4π	single slice	2.20	—	2.20	—
	20%	3.76	0.72	4.20	0.88
	100%	3.41	0.42	3.42	0.42

±2π or ±4π.

The phase angle dispersions for different gaps are shown in Table 4. When the gap was set to 100%, the phase angle dispersion decreased. Similar to the findings for the in-plane signal value, for either gap, the phase angle dispersion at ±3π approached the single-slice phase angle dispersion.

3.3 Results for Mxy slice profiles at the echo peak time

The results for acquisition with different NS values and slice excitation orders at ±2π, ±3π, and ±4π are shown in Figures 2, 3, and 4, respectively.

In interleaved acquisition, the Mxy slice profiles of odd-numbered slices did not appear to deteriorate at any π value, but the Mxy slice profiles of even-numbered slices deteriorated at all π value. The degree of deterioration was the same at all π values. On the other hand, in sequential acquisition, the Mxy slice profiles from the 2nd slice to the 13th slice showed deterioration at all π values. The degree of deterioration was the same from the 2nd slice through the 13th slice.

The deterioration showed the same characteristics for both interleaved acquisition and sequential acquisition. At ±2π, the center of the Mxy slice profile showed severe deterioration, and at ±3π and ±4π, deterioration was observed not at the center of the Mxy slice profile but at both ends. In particular, in sequential acquisition, deterioration was observed on only the right side of the Mxy slice profile at ±3π and ±4 π.

For both interleaved acquisition and sequential acquisition, the deterioration of the Mxy slice profiles was unaffected by changes in NS, but was increased when the gap was larger.

4. Discussion

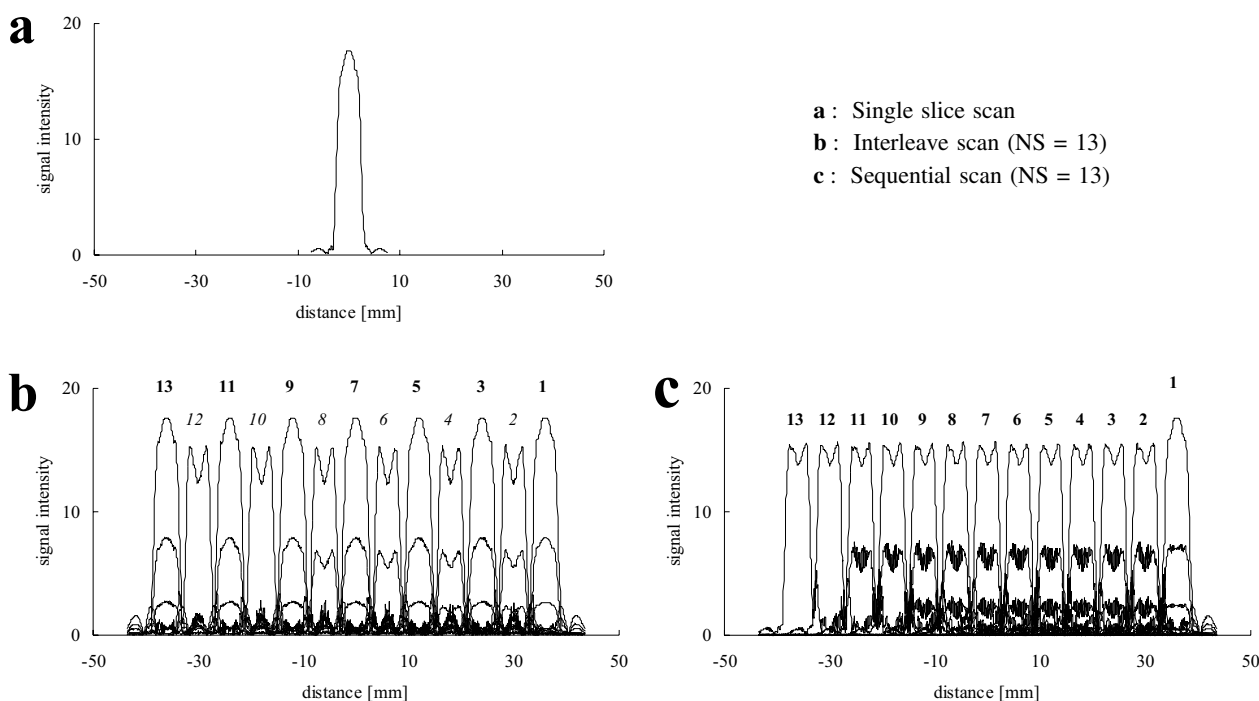In the present study, we performed numerical analysis under

a : Single slice scan
b : Interleave scan (NS = 13)
c : Sequential scan (NS = 13)

Fig.2 Slice profile for ±2π (gap = 20%). The odd-numbered slices in interleaved acquisition show the same slice profile shape as a single slice. The even-numbered slices show deterioration at the center of the slice profile. In sequential acquisition, the first slice is the same as a single slice, but the slices after the 2nd show similar deterioration at the center of the slice profile.
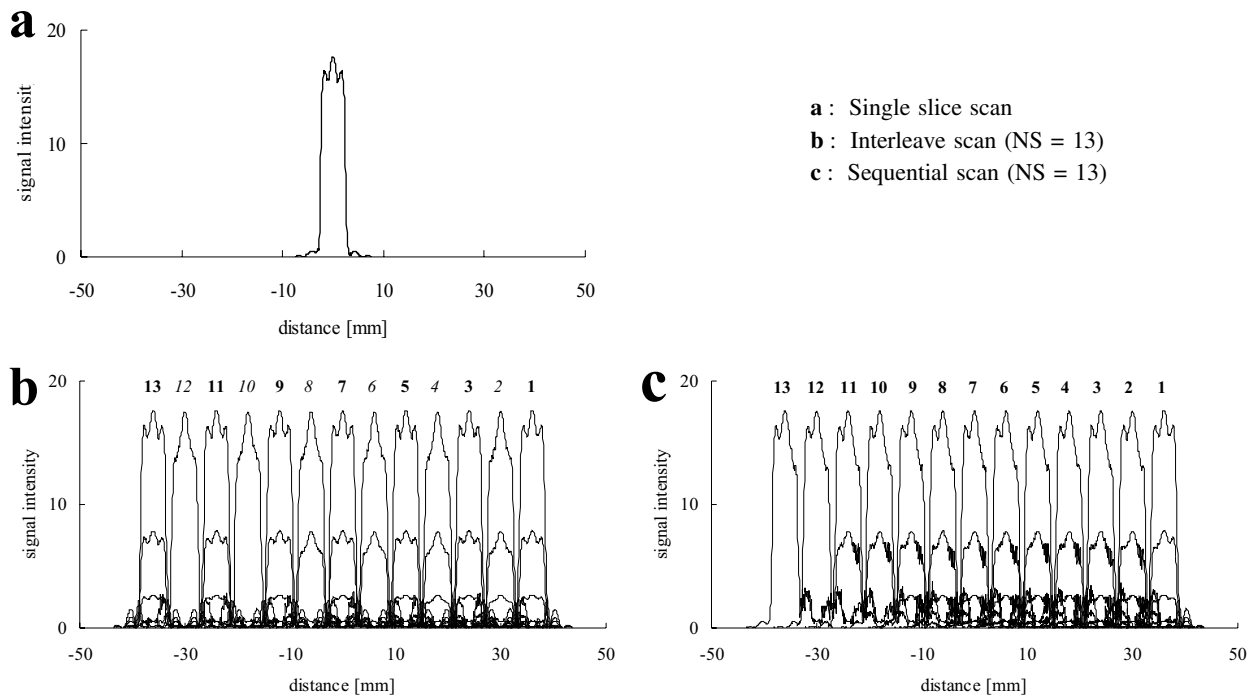
Fig.3 Slice profile for ±3π (gap = 20%). The odd-numbered slices in interleaved acquisition show the same slice profile as a single slice. The even-numbered slices show deterioration at the center and on the right and left sides of the slice profile. In sequential acquisition, the first slice is the same as a single slice, but the slices after the 2nd show similar deterioration of the slice profile (i.e., only on the right side).
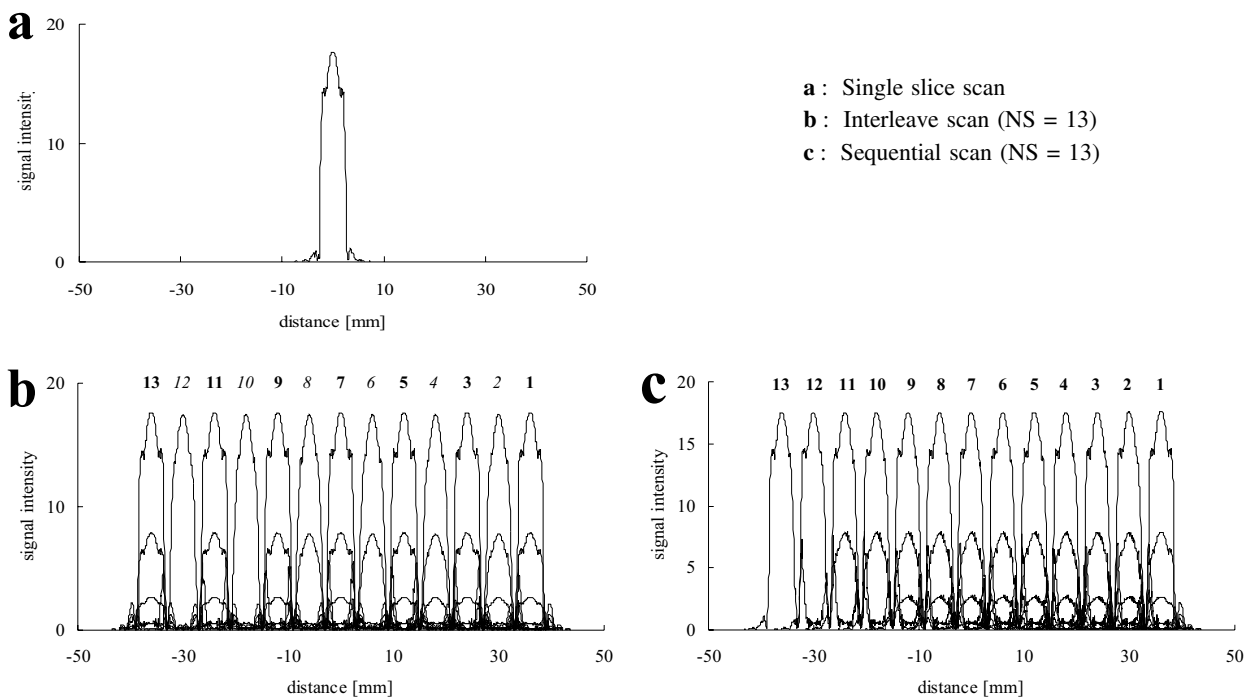

Fig.4 Slice profile for ±4π (gap = 20%). The deterioration of the slice profile shows the same characteristics at ±4π and ±3π.

ideal conditions using the Bloch equation and conducted simulation analysis of the signal intensities of multislice data obtained using various acquisition parameters.

With regard to the effects of the number of slices NS, theoretical numerical simulation was able to confirm the in-plane signal value is smaller than single-slice for the NS ≥ 2. Comparing interleaved acquisition and sequential acquisition, for all NS

value, the SD of in-plane signal value was larger in interleaved acquisition. This means that there is interslice sensitivity variation. In addition, this large SD is attributable to differences in the in-plane signal values between the odd-numbered and even-numbered slices in interleaved acquisition.

Interleaved acquisition is generally considered not to be susceptible to crosstalk interference. However, when the gap

was set to narrow in interleaved acquisition, the interslice sensitivity variation due to differences in the in-plane signal value and phase angle dispersion were observed between the odd-numbered and even-numbered slices.

The results of echo peak time Mxy slice profile evaluation showed that the shape of the Mxy slice profile differed between the odd-numbered slices and the even-numbered slices in interleaved acquisition. This result in differences in the in-plane signal value, which was thought to cause interslice sensitivity variation between the odd-numbered slices and the even-numbered slices. On the other hand, in sequential acquisition, the Mxy slice profile showed similar shape from the 2nd slice through the 13th slice. Therefore, sequential acquisition was thought to show almost no interslice sensitivity variation from the 2nd slice through the 13th slice. In terms of the degree of degradation, both interleaved acquisition and sequential acquisition showed severe deterioration at the center of the Mxy slice profile at $\pm 2\pi$. This was thought to be the reason that the in-plane signal value of $\pm 2\pi$ was smaller than $\pm 3\pi$ and $\pm 4\pi$.

When NS was 13 and gap was 20% in sequential acquisition, $\pm 3\pi$ showed improved in-plane signals as compared with $\pm 2\pi$ or $\pm 4\pi$ (5.83% and 1.04% improvement, respectively) as well as improved phase angle dispersion (22.86% and 20.00% improvement, respectively).

Based on the above findings, multislice simulation under ideal conditions using the Bloch equation suggests that sequential acquisition with the RF pulse π value set to $\pm 3\pi$ is suitable for minimizing interslice signal variation.

5. Summary

Multislice acquisition is currently employed as the standard in MRI studies, but this method is generally associated with lower signal intensities than single-slice acquisition. This is thought to be attributable to crosstalk interference due to deterioration of the rectangular profile of the excitation RF pulse shape. This problem can be avoided either by setting a gap between slices or by employing interleaved acquisition in which the multislice excitation order is changed. However, few reports have described how the acquisition parameters affect the slice profiles in multislice acquisition. In the present study, we performed simulation analysis of SE multislice signal intensities under ideal conditions. The RF pulse shapes employed were symmetrical sinc $\pm 2\pi$, $\pm 3\pi$, and $\pm 4\pi$. The targets of the analysis were the Mxy in-plane signal value and variance value

and the Mxy slice profile in the echo time. It was found that sequential acquisition showed less variance in the in-plane signal values and less interslice sensitivity variation than interleaved acquisition. In addition, multislice evaluation of 13 slices showed that the $\pm 3\pi$ slice profile was closest to a single slice, and its in-plane signal value was also close to that of a single slice. In conclusion, $\pm 3\pi$ sequential acquisition is able to improve in-plane signal values and variance values as compared with $\pm 2\pi$ and $\pm 4\pi$.

References

[1] Pauly J, Le Roux P, Nishimura D, et al.: Parameter relations for the Shinnar-Le Roux selective excitation pulse design algorithm. IEEE Transactions on Medical Imaging 10(1), 53-65, 1991.

[2] Filippi M, Yousry TA, Rocca MA, et al. : The effect of cross-talk on MRI lesion numbers and volumes in multiple sclerosis using conventional and turbo spin-echo. Multiple Sclerosis 4(6), 471-474, 1998.

[3] Slavin GS, Rettmann DW: Addressing efficiency and residual magnetization cross talk in multi-slice 2D steady-state free precession imaging of the heart. Magn. Reson. Med. 53(4), 965-969, 2005.

[4] Bernstein MA, King KF, Zhou XJ : Handbook of MRI Pulse Sequences. 410-413, Elsevier Academic Press, 2004.

[5] Bloch F: Nuclear induction. Phys. Rev. 70, 460-474, 1946.

[6] Hinshaw WS, Lent AH: An introduction to NMR imaging: From the Bloch equation to the imaging equation. Proceedings of the IEEE 71, 340-345, 1983.

[7] Olsson MB, Wirestam R, Persson BR: A computer simulation program for MR imaging : Application to RF and static magnetic field imperfections. Magn. Reson. Med. 34(4), 612-617, 1995.

[8] Runge VM, Wood ML, Kaufman DM, et al.: MR imaging section profile optimization: Improved contrast and detection of lesions. Radiology 197, 831-834, 1988.

[9] Henkelman RM, Bronskill MJ: Artifacts in magnetic resonance imaging. Rev. Magn. Reson. Med. 2, 1-126, 1987.

[10] Zur Y, Stokar S : A phase-cycling technique for canceling spurious echoes in NMR imaging. J. Magn. Reson. 71, 212-228, 1987.

[11] Partain CL, Price RR, et al.: Magnetic Resonance Imaging. Saunders, 1082, 1988.